Med Biol Eng Comput (2013) 51:103–112
DOI 10.1007/s11517-012-0973-x

ORIGINAL ARTICLE

Self-mixing microprobe for monitoring microvascular perfusion in rat brain

Edite Figueiras · Ricardo Oliveira · Cátia F. Lourenço · Rita Campos · Anne Humeau-Heurtier · Rui M. Barbosa · João Laranjinha · Luis F. Requicha Ferreira · Frits F. M. de Mul

Received: 30 May 2012 / Accepted: 28 September 2012 / Published online: 12 October 2012

Abstract Measuring functional activity in brain in connection with neural stimulation faces technological challenges. Our goal is to evaluate, in relative terms, the real-time variations of local cerebral blood flow in rat brain, with a convenient spatial resolution. The use of laser Doppler flowmetry (LDF) probes is a promising approach but commercially available LDF probes are still too large (450 μm) to allow insertion in brain tissue without causing damage in an extension that may negatively impact local measurements. The self-mixing technique coupled to LDF is herein proposed to overcome limitations of the minimal diameter of the probe imposed by non-self-mixing probes (commercial available probes). Our Monte Carlo simulations show that laser photons have a mean penetration depth of 0.15 mm, on the rat brain with the 785 nm laser light microprobe. Moreover, three self-mixing signal processing methods are tested: counting method, autocorrelation method, power spectrum method. The perfusion signal computed shows a good linearity with the scatterers velocity, for the three methods (a determination coefficient close to one is obtained), for the in vitro measurements. Furthermore, we believe that these indicators can be used to monitor local blood flow changes in the rat brain.

Keywords Self-mixing · Laser Doppler flowmetry · Blood flow · Microcirculation

E. Figueiras (✉) · R. Oliveira · R. Campos · L. F. Requicha Ferreira
Instrumentation Center (GEI-CI), Physics Department, Faculty of Sciences and Technology of Coimbra University, Rua Larga, 3004-516 Coimbra, Portugal
e-mail: editefigueiras@gmail.com

C. F. Lourenço · R. M. Barbosa · J. Laranjinha
Center for Neurosciences and Cell Biology (CNC), University of Coimbra, Largo Marquês de Pombal, 3004-517 Coimbra, Portugal

A. Humeau-Heurtier
LISA, Laboratoire d'Ingénierie des Systèmes Automatisés, LUNAM Université, Université d'Angers, 62 Avenue Notre Dame du Lac, 49000 Angers, France

R. M. Barbosa · J. Laranjinha
Faculty of Pharmacy of Coimbra University, Health Sciences Campus, Azinhaga de Santa Comba, 3000-548 Coimbra, Portugal

F. F. M. de Mul
Department of Applied Physics, Biomedical Optics Group, University of Twente, Enschede, The Netherlands

1 Introduction

1.1 Basic principles and measuring system

Laser Doppler flowmetry (LDF) is a technique to monitor microvascular blood perfusion in real time. The principles of this technique encompass the use of a coherent laser light beam carried from a laser unit by an emitting optical fibre to the tissues under study [2, 6]. The light is then reflected, scattered, absorbed or transmitted in the tissues. When photons hit moving red blood cells (RBCs), a change in their wavelength occurs (Doppler shift), conversely to the photons that hit static structures that do not have any modification in their wavelength [2, 6]. The magnitude and frequency distribution of the wavelength changes are directly related to the number and velocity of the RBCs in the sampled volume [6]. A receiving fibre guides the backscattered Doppler shifted and non-Doppler shifted photons to a photodetector, where they are mixed, and converted into an electrical signal for electronic processing

[12]. In this configuration, two optical fibres are needed that entail positioning and alignment of individual optical components in the probe.

Self-mixing interferometry has been used in LDF since the earliest 90s [11, 12, 25]. Self-mixing detection in LDF relies on the phenomenon that occurs in a semiconductor laser diode when a relatively small part of the emitted laser light is coupled back into the laser cavity. The returned Doppler shifted photons interfere with the laser light inside the laser cavity causing an intensity modulation of the laser light [10]. This Doppler frequency shift carries information on the distance, velocity, and surface of the target. It can be measured as a signal component in the pump current of the laser or as a signal of a monitor photodiode, which is frequently positioned at the backside of the laser for laser light power monitoring [22]. Contrary to conventional LDF measurement systems, in self-mixing interferometry, only one optical axis is needed since the source and detection planes are along the same optical axis. Besides this, single mode optical fibres (which have small diameters) can be used, which facilitates the use of small catheters for invasive measurements [25]. This technique eliminates the need of additional detectors and components such as isolators and pinholes. This leads to cheaper and more compact systems [20].

1.2 Brain microcirculation and motivation

Brain requires a continuous vascular supply of glucose and oxygen to sustain a proper function, given that neurons lack substrate storage, high metabolic rate and high sensitivity to oxygen deprivation. Furthermore, the supply of blood flow-carrying substrates must be locally and dynamically regulated to meet the energetic demand associated with the increase of the neuronal activity. The existence of mechanisms that incorporate variations in neuronal activity with local blood supply was firstly suggested more than a century ago but they are still not fully clarified. This is a critical process for brain structural and functional integrity [7]. LDF is an increasingly used technique for real-time assessment of cerebral blood flow changes and for the study of the mechanisms by which brain controls its own blood supply [7]. Because of its small sample volume ($\sim$1 mm^3), LDF has a reasonable spatial resolution to be used in the investigation of the mechanisms that regulates cerebral hemodynamics [26]. In microcirculatory brain blood flow measurements, LDF is primarily considered a non-invasive technique mainly used in studies of hemodynamic events in cortical surfaces [4, 14].

The available commercial LDF probes are based on the traditional detection method where two optical fibres (an emitting and a receiving fibres) are needed, restricting the minimum diameter of the probes around to c.a. 500 µm. Therefore, the development of smaller probes, allowing the monitoring of blood flow changes in deep brain structures minimising tissue damage and the negative impact over natural environment, is an important requirement to better understand how brain controls its own blood supply. Thus, to monitor blood flow changes in deep brain structures, we propose to develop a miniaturized LDF probe based on a self-mixing method [16].

In vitro and in vivo validations of the self-mixing prototype are presented in this paper. Several signal processing methods were proposed in the literature for self-mixing signals processing, namely the counting method (CM), the autocorrelation method (AC) and the power spectrum method (PSM) [19, 20]. These methods will be evaluated for both in vitro and in vivo validations. A discussion of the effects of the signal processing methods on the results is presented together with a comparison of the results obtained with the microprobe prototype and with a commercial available flowmeter.

2 Methods

2.1 Self-mixing prototype

A laser Doppler flowmeter prototype with self-mixing capabilities, outlined in Fig. 1, is being constructed in our laboratory and validated for rat brain invasive measurements [16]. The prototype is formed by the actuation system, represented in Fig. 1a, and the self-mixing acquisition system, represented in Fig. 1b. The actuation system has two constant current drivers for two different lasers diodes. The acquisition system is responsible for the self-mixing photocurrent amplification and the digitalization of the detected signal through the NI-USB 6210 (National Instruments®). Matlab® routines and subroutines are used for mathematical analyses. The PIC24FJ128GA010 from

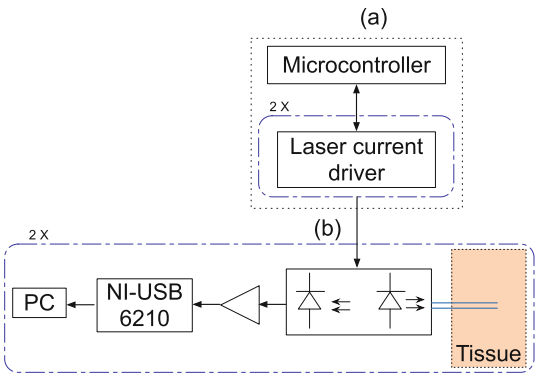

Fig. 1 Prototype schema: **a** actuation system; and **b** self-mixing acquisition system

Microchip is used for switching the control of the lasers and for current laser monitoring [16].

Pigtailed laser diodes with a single mode optical fibre are used. Two semiconductor laser diodes with different wavelengths are proposed: one with a 785 nm wavelength (model: DL-7140-001S) with an optical power of 70 mW at the operating current (100 mA) and the other with a 1,308 nm wavelength (model: QLD 1300-50S) with an optical power of 50 mW at the operating current (137 mA). Both wavelengths are in the diagnostic window range (600–1,600 nm) [15]. The single mode optical fibre has a cladding diameter of 125 μm that was fixed inside a microneedle to allow robustness of the probe and stability of the acquired signal, since the movement or vibration of the fibre affects the output signal [28, 29].

2.2 Monte Carlo simulations

The Monte Carlo algorithm used was developed by Frits de Mul and is described elsewhere [13]. Monte Carlo simulations were performed in order to determine the mean depth travelled by the Doppler shifted photons in rat brain tissue. Thus, a simulation model of the rat brain hippocampus has been built based on the works of Fredriksson et al. [3] and Hamberg et al. [5]. The rat hippocampus consists of gray matter, white matter and blood vessels, among others. The blood percentage is nearly 4.5 % and the white matter is up to 4 % of the blood volume. As the percentage of white matter is very low, we considered that the hippocampus has 95.5 % of gray matter and 4.5 % of blood (3.6 % of oxygenated blood and 0.9 % of deoxygenated blood) [3, 5].

The optical properties chosen in the simulations for the 785 nm wavelength were based on Ref. [3]. The absorption coefficients used were 0.2, 0.5 and 0.64 mm^{-1} for gray matter, oxygenated and deoxygenated blood, respectively. The scattering coefficients were 0.78 mm^{-1} for the gray matter and 2 mm^{-1} for oxygenated and deoxygenated blood and the anisotropy factor was 0.900 for gray matter and 0.991 for oxygenated and deoxygenated blood [3]. Concerning the scattering functions, the blood (oxygenated and deoxygenated) was modelled with the Gegenbauer kernel scattering phase function, with $\alpha = 1$ and $g = 0.948$ mm^{-1} [3]. For gray matter, the Henyey–Greenstein phase function was used with $g = 0.85$ mm^{-1} [3]. For blood, a haematocrit equal to 42 % was considered. The refractive index was set to 1.4 to all components and the laser light was simulated as a pencil beam with a perpendicular entrance in the tissue. The path tracking was recorded with $1/\mu$ resolution, where μ is the reduced scattering coefficient. The numerical aperture (NA) of the optical fibres was 0.11.

The simulations were performed only for the 785 nm laser light wavelength due to the absence of information concerning optical properties of gray matter, oxygenated and deoxygenated blood for the 1,308 nm laser light beam.

2.3 Validation tests

2.3.1 In vitro measurements

A mechanical apparatus mimicking a rotating turntable was developed in order to test and verify the linearity of our system for different scattering velocities. It consists of an aluminium plate coupled to a DC motor. The microprobe was positioned close to perpendicular to the plate, at less than 1 mm from the aluminium surface, with micrometric controllers that allow a good positioning between the probe and the moving target. A set of 12 velocities were tested between 0 and 48 mm/s. A continuous acquisition was made, where the moving target was moving at each velocity during 2 min.

2.3.2 In vivo measurements

In vivo tests were performed in male Wistar rats (9 weeks). Rats were anesthetized with urethane (1.25 g/kg, i.p.), and placed in a stereotaxic frame (Stoelting Co, USA). After the animal was properly fixed, an anterior/posterior incision was done on the midline of the scalp and the skin folded back. Under a stereo microscope (Meiji EMZ13, Japan), the anatomical landmark, bregma, was identified. A small portion of the skull ($\sim 3 \times 4$ mm) overlying the hippocampus was removed by using a small hand drill. After removing, carefully, the portion of drilled bone, the overlying "dura mater" was pulled off using thin tip forceps to expose the brain surface and to allow the probe penetration. The microprobe (785 nm or 1,308 nm laser) was stereotaxically inserted into the hippocampus according to coordinates. These calculations were based on a rat brain atlas [23]. Together with our probe, we inserted a commercial laser Doppler, using a two optical fibres needle probe (Perimed reference: PF411; outer diameter, 450 μm; fibre separation, 150 μm; wavelength, 780 nm) connected to a laser Doppler flowmeter device (Periflux system 5000, Perimed, Sweden), in the opposite cerebral hemisphere. Different brain tissue damages are associated with the different probe sizes. This is not important because we have used the commercial flowmeter probe as a control to our prototype, only.

Measurements were made with both wavelengths (1,308 and 785 nm) in different animals. After the probes implantation, a baseline was recorded during c.a. 5 min and then sodium nitrite (200 mg/kg in saline solution) was intraperitoneally injected, in order to induce metahemoglobinemia and finally cardiac arrest.

The correlation between the results obtained with the Perimed probe and with both microprobes was computed.

The signals were normalised before the cross-correlation computation.

2.4 Signal processing

Typical speckle signals obtained at 6 and 48 mm/s on the mechanical phantom can be seen in Fig. 2. Both signals were sampled at 50 kHz. The intensity fluctuations of the speckle signal at 48 mm/s are higher than the intensity fluctuations of the speckle signal at 6 mm/s which proves that the self-mixing signal contains velocity information.

In vitro and in vivo signals were sampled at 50 kHz and they were processed with a frequency rate of 32 Hz with a 3 dB cut-off frequency of 7.5 Hz. The frequency rate and the low cut-off frequency are in accordance with the values used by commercial flowmeters (for e.g., Periflux 5000 from Perimed).

The CM, the AM, and the PSM are evaluated thereafter because there is no standard method for self-mixing signal processing.

2.4.1 Counting method

The CM consists in converting the speckle signal into a pulse train signal in order to calculate the speckle frequency. The signal is compared with a threshold level that produces a binary pulse train depending on the result of the comparison. If the intensity values are less than this threshold level, the output of the comparator is 0; if the intensity values are above the threshold, it is 1. The resulting signal is the binary pulse train. The number of pulses during a measuring time is the speckle frequency which is related with the velocity of the moving object [18, 19, 22]. A pulse train obtained from the speckle signal can be seen in Fig. 3. The speckle frequency gives information about the power spectral density of the speckle signal, as it

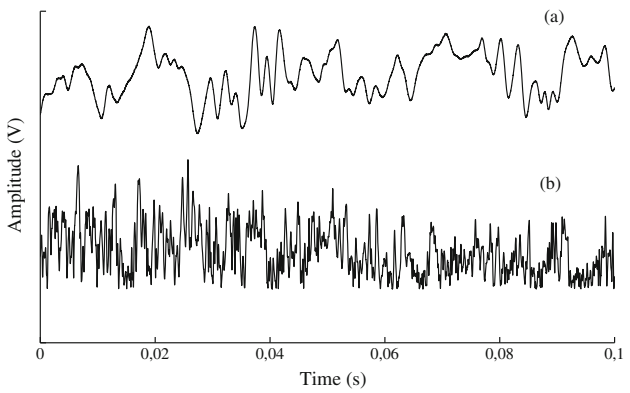

Fig. 2 Speckle signals obtained on the phantom for: **a** 6 mm/s and **b** 48 mm/s with the 1,308 nm laser diode. As the two signals have the same mean voltage, the amplitude of the signals was changed to facilitate the visualisation

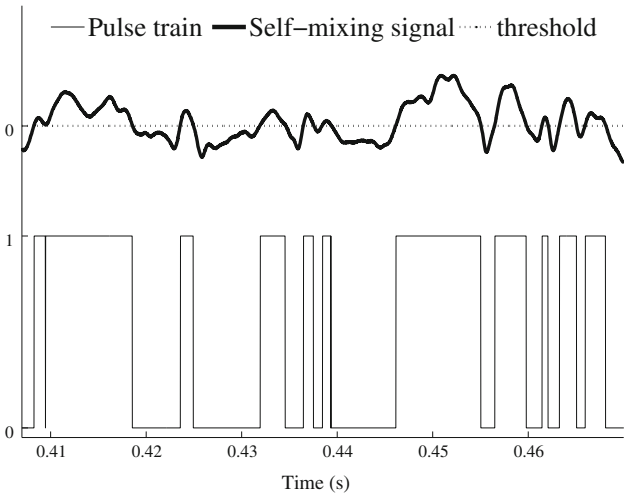

Fig. 3 Speckle signal waveform and the converted pulse trains obtained with the turntable at velocity of 6 mm/s, with the 1,308 nm laser diode

is an estimation of the frequency content of the speckle signal [18].

The signal acquired was divided into blocks of a predetermined time interval size before the binary pulse train conversion. The size of the blocks was defined in order to obtain a processed signal with a frequency rate of 32 Hz. The frequency rate is defined as the number of processed points obtained per second and can be obtained as:

$$\text{Frequency rate} = \frac{f_s}{\text{npts} \times (1 - \text{overlap})} \quad (1)$$

where f_s is the sampling frequency, npts the number of points used in each block and overlap is the (overlap in percent)/100. A f_s of 50 kHz, a npts of 2,048 and an overlap of approximately 24 % yield a frequency rate of 32 Hz. Denoting the number of such fluctuations in each block of duration t as N, the speckle frequency is calculated as $f_{\text{speckle}} = N/t$.

Before the binary pulse train calculation, the DC component of each block was subtracted. Moreover the threshold was defined as 0.01 and 0.001 V for 1,308 and 785 nm laser diode, respectively, for phantom measurements. It was defined as 0.005 and 0.003 V for 1,308 and 785 nm laser diode, respectively, for rat brain measurements. A moving average with 20 points was applied to the processed signals in order to improve the visualisation.

2.4.2 Autocorrelation method

The autocorrelation function and the power spectral density form a Fourier pair in accordance with the Wiener–Khintchin theorem. As it has been shown before, the power spectral density and the speckle frequency contain velocity information of the moving scatterers. Therefore, it is clear

that careful processing of the autocorrelation function can also give information about the velocity of the target [17]. Figure 4 shows the behaviour of the autocorrelation for signals collected in the mechanical phantom. The signals were acquired at 50 kHz and the autocorrelation function was computed for 2,048 points. A mean autocorrelation function was calculated for 2 min of signal acquisition. It can be easily noted that the time of decay increases with the decrease of the target velocity for both laser diodes (Fig. 4a, b) but it is more clear for 1,308 nm laser light.

The AM is based on computing the time when the autocorrelation function drops to a fraction of its maximum value. This time is called the autocorrelation time, τ [22]. Then the reciprocal of the autocorrelation time is computed. For the in vitro measurements, the drop was defined as $1/e$ and 0.85 for 1,308 and 785 nm, respectively, whereas, for in vivo measurements, it was defined as $1/e$ for both laser diodes. For the in vivo results, the autocorrelation function was normalised to the first lag because the difference between the zero lag and the other lags was very high which made the choice of the drop threshold. To improve the visualisation of the AM results, for the in vivo validation, the absolute value of the differences between adjacent elements of the processed signals were computed and a moving average with 20 points was applied.

As in the CM, the speckle signal was divided into blocks, with an overlap of approximately 24 %, with 2,048 points. Then, the autocorrelation was computed for each block and finally the autocorrelation time was computed.

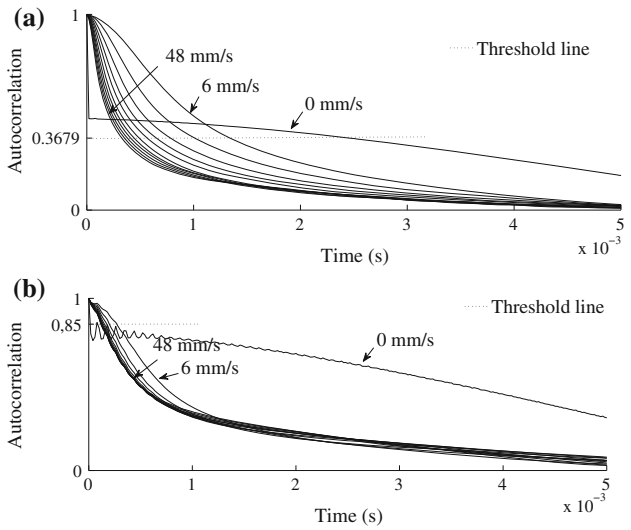

Fig. 4 Normalised autocorrelation functions obtained for a: **a** 1,308 and **b** 785 nm laser diode for 0, 6, 10, 14, 19, 23, 27, 31, 35, 40, 44 and 48 mm/s in the mechanical phantom. The autocorrelation decay time increases with the decrease of the target velocity for both laser diodes. The threshold line cuts the graphs when each function drops to $1/e$ in **a** and to 0.85 in **b**

2.4.3 Power spectrum method

In the PSM, the power spectral density is computed to have information on the frequency components of the signal and to assess its nature. The photocurrent power spectrum is related with the properties of the moving targets in the illuminated volume. The moments of the power spectrum, $P(f)$, of the speckle signal are given by:

$$M_i = \int \omega^i \times P(\omega)\, d\omega \tag{2}$$

where M_i is the ith order moment of the power spectral density and f is the frequency components [1].

It has been shown, for the conventional LDF measurement systems (non-self-mixing configuration), that the concentration of moving blood cells (CMBCs) and the perfusion can be estimated from the power spectrum [1]. The CMBC is proportional to the integral of the Doppler power spectrum density, M0 [1]:

$$\text{CMBC} = \int P(\omega)\, \mathrm{d}\omega \tag{3}$$

and the perfusion is proportional to the integral of the frequency weighted Doppler power spectrum, M1 [1]:

$$\text{Perfusion} = \text{CMBC} \times \langle v \rangle \propto \int \omega P(\omega)\, \mathrm{d}\omega \tag{4}$$

where $\langle v \rangle$ is the mean speed of the blood cells.

To our knowledge, a theoretical analysis of self-mixing signals from living tissues has not been developed yet due to the complicated structure of the self-mixing effect and the living tissues [19]. Despite that, M0 and M1 will be evaluated as M1 was previously evaluated by other authors [25, 27].

Power spectra obtained for 0, 6, 10, 14, 19, 23, 27, 31, 35, 40, 44 and 48 mm/s, in the mechanical phantom can be seen in Fig. 5. Only the lowest frequencies of the spectra are shown to improve the visualisation. The signals were acquired at 50 kHz and the power spectra were computed for 2,048 points. A mean spectrum was calculated for 2 min of acquisition and a low cut-off frequency of 2 kHz was used for both laser lights in the in vitro validation. The low cut-off frequency was chosen based on the observation of the spectra (Fig. 5). The increase in the broadening of the spectra is more clear for 1,308 nm laser light (Fig. 5a) than for 785 nm laser light (Fig. 5b).

For the in vivo validation, 25 Hz and 16 kHz were chosen as low and high cut-off frequency, respectively. The low cut-off frequency was chosen equal to 25 Hz in order to eliminate contributions from the DC component (non-Doppler shifted light) in the signal [9]. The upper limit is related with the maximum frequency shift that can be expected for blood microcirculation measurements, that

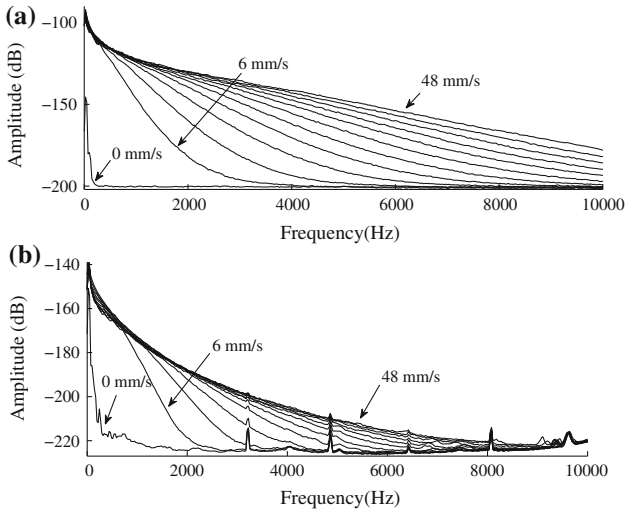

Fig. 5 Power spectra obtained for a: **a** 1,308 and **b** 785 nm laser diode for 0, 6, 10, 14, 19, 23, 27, 31, 35, 40, 44 and 48 mm/s in the mechanical phantom with the broadening of the spectra increasing with the velocity

is 25 kHz. However, the average shift is much lower due to multiple scattering events and the fact that the moving RBCs do not have all the same velocity. So, the spectrum will have an approximately exponential decay that does not exceed 16 kHz. A moving average of 20 points was applied to M0 results for visualisation improvement.

Considering that the perfusion rate, determined by:

$$\text{Perfusion rate} = \frac{f_s}{\text{nfft} \times (1 - \text{overlap})} \tag{5}$$

where nfft is the number of points of the PSD, a nfft of 2,048 and an overlap of 24 % were needed, in order to obtain a frequency rate of approximately 32 Hz.

3 Results

3.1 Monte Carlo results

The simulations performed for the model shows that the Doppler shifted photons travelled a mean depth of 0.15 mm in the hippocampus region. Each photon suffers in average 2.23 scatters events. In a total of 5,000,000 photons detected, 11.9 % had suffered Doppler shifts.

3.2 In vitro results

The results of the three signal processing methods are plotted versus the velocity in Fig. 6. Figure 6a, c, e and g shows the results obtained with 1,308 nm laser light for CM, AM, M0 and M1, respectively, whereas Fig. 6b, d, f and h shows the results obtained with 785 nm laser light for CM, AM, M0 and M1, respectively. A linear regression was performed, where the results were fitted to a first order polynomial, in order to validate the linearity of the system.

In the AM and in the CM for 785 nm laser diode, the result obtained for 0 mm/s was not used for the linear regression study. The statistical analysis shows good correlation between the fitted model and the results since the coefficient of determination, R^2, is higher than 0.9, except for AM with a 785 nm laser light ($R^2 = 0.88$). Moreover, the p value is lower than 0.01. Therefore, we can conclude that, in general, the relation between the results of the processing methods and the velocity are linear.

3.3 In vivo results

The signals collected in the rat brain were processed and compared with those obtained with the Perimed probe. All the above-mentioned signal processing methods were tested. Cerebral blood flow variations were promoted by systemic injection of sodium nitrite, which induces a biphasic effect over blood perfusion: (i) soon after the injection, blood perfusion slightly increases due to nitrite-induced vasodilatation [24] and later in consequence of cardiac output rise (to balance the decreased oxygen transport due to metahemoglobinemia), and (ii) finally, an abrupt decrease is observed due to cardiac arrest.

Signals were collected from several animals (6 measurements with M1308 and 5 measurements with M785). We only show signals collected in two of those: one acquisition was made with the 1308 nm laser light wavelength (M1308) and the other with the 785 nm laser light wavelength (M785). Similar results were obtained in the remaining animals. The Periflux 5000, CM, AM, M0 and M1 results are presented in Figs. 7 and 8 for M1308 and M785, respectively.

In M1308 measurements, three regions can be seen in the signals amplitude for Periflux 5000, CM, AM and M0 results (see Fig. 7). An initial baseline can be seen during the first 5 min of acquisition, followed by an increase in the amplitude and its oscillations. Finally, the amplitude decreases after 25 min of acquisition during the cardiac arrest (see Fig. 7). For the M1 results, a pattern that changes in accordance with these three regions can be seen. The maximal perfusion that occurs after the nitrite injection was detected at 21.18, 18.22, 19.26 and 22.12 min in Periflux 5000, CM, AM and M0, respectively. The increase percentage, between the mean baseline value and the peak, was 32.6, 69.45, 74.72, 74.20 % in Periflux 5000, CM, AM and M0, respectively.

In M785, an initial baseline can be seen during the first 5 min in Periflux 5000, CM, AM and M0 results (see Fig. 8). After the nitrite injection, the mean amplitude decreases in Periflux 5000. This could be due to a probe

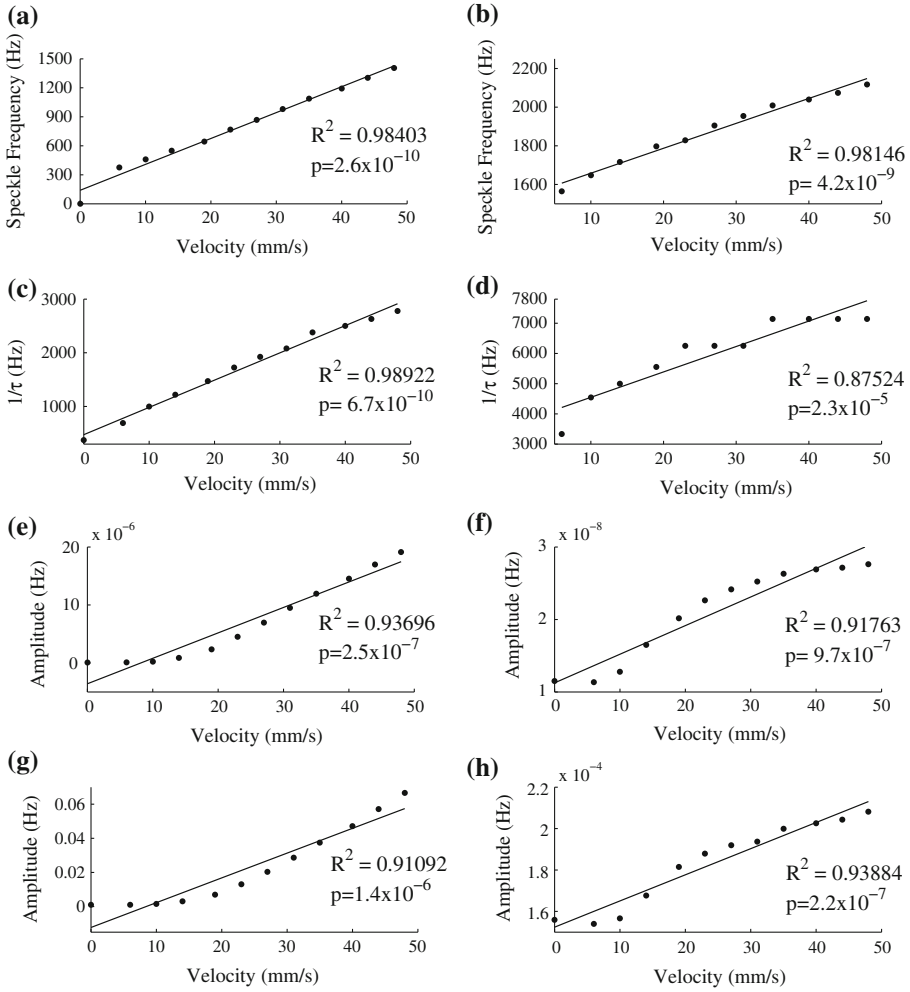

Fig. 6 In vitro validation results: **a** CM, **c** AM, **e** M0 and **g** M1 obtained with 1,308 nm laser light; **b** CM, **d** AM, **f** M0 and **h** M1 obtained with 785 nm laser light

displacement during the nitrite injection. Despite that, the perfusion increases in the next 19 min followed by an amplitude oscillation and finally the amplitude decreases after 27 min of acquisition during the cardiac arrest in Perimed, CM, AM, M0 and M1 results (see Fig. 8). The maximal perfusion that occurs after the nitrite injection was detected at 25.43, 22.30, 23.12, 24.50 and 24.50 min in Periflux 5000, CM, AM, M0 and M1, respectively. The increase percentage was 19.10, 69.85, 70.25, 66.17 and 31.3 % in Periflux 5000, CM, AM and M0, respectively. A peak registered in Perimed at 28 min, caused by cardiac arrhythmias, can also be seen in the results obtained in our prototype (see Fig. 8).

4 Discussion

The measurement depth obtained in Monte Carlo simulations is in accordance with the one of Fredriksson et al. [3] where the authors reported a 0.16 mm of measurement depth. These results are useful for the rat brain probe positioning, since the position of the probe in the specific region of the hippocampus is conditioned by the mean depth travelled by the Doppler shift photons.

Monte Carlo simulations for 1,308 nm were not implemented, as optical properties for biological tissues are published only up to 1,000 nm wavelength. Despite that, for this wavelength, it is necessary to consider the water present in the tissue, as the absorption coefficient is high (for 1,300 nm, the absorption coefficient of water is 1.35 cm^{-1}) when compared with visible and near infra-red wavelengths (for 785 nm, the absorption coefficient of water is 0.02398 cm^{-1}) [8]. This implies that, when we consider the 1,308 nm laser light, most of the light is absorbed by water, so the incident beam will only penetrate a few cell diameters into the tissue [15].

In the signals collected in the rotating turntable, a lower drop of the maximum value of the AM was used for 785 nm in the phantom measurements: as it can be seen in Fig. 4b, the autocorrelation functions of different velocities for larger lag times mix, loosing the velocity information. Besides that, the results obtained for 0 mm/s was discarded

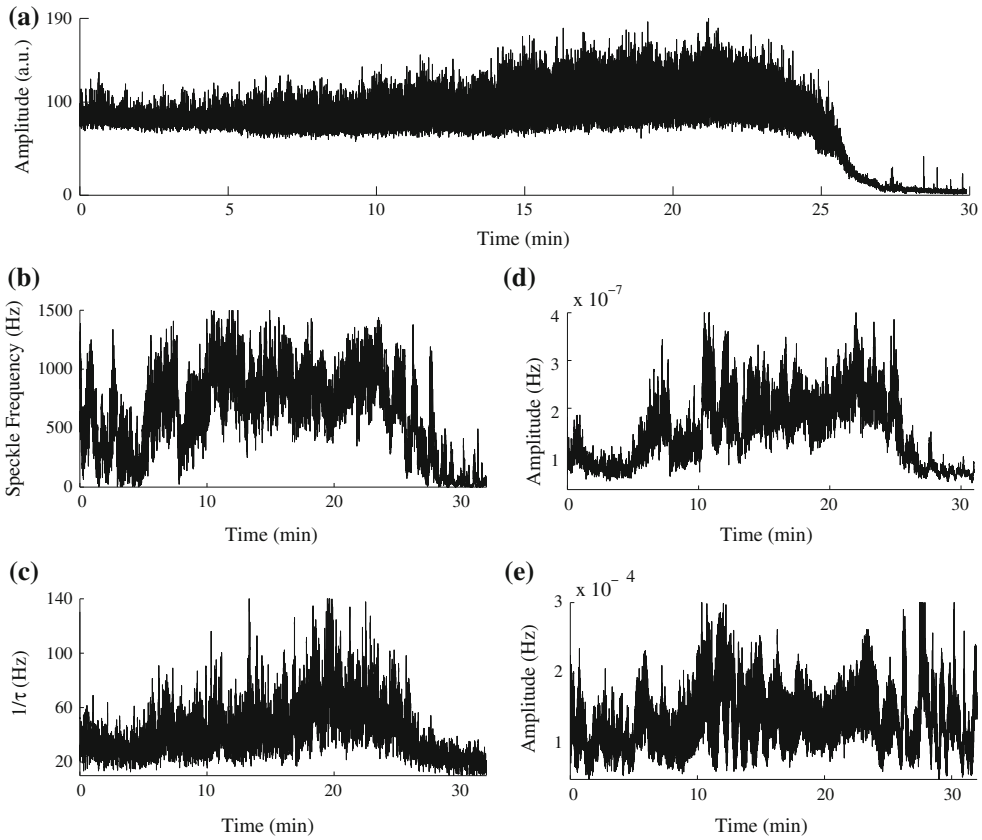

Fig. 7 In vivo validation results for M1308: **a** Periflux 5000 results, **b** CM results, **c** AM results, **d** M0 results and **e** M1 results

from the statistical analysis. As it can be seen in Fig. 4b, the autocorrelation function for 0 mm/s has a very different shape when compared with the other velocities. The autocorrelation function for 0 m/s has a very slow decay time when compared with the other velocities; however, for the lower lag times it has a faster decay. The drop threshold was chosen in this fast decay region. That is why the AM result for this velocity is out of the range of the results obtained for the other velocities.

Concerning the CM results, a set of thresholds were tested. The ones with the best results were chosen for in vitro and in vivo validation. In the PSM results, in the in vitro tests, a higher low cut-off frequency was chosen (2 kHz) based on the observation of the spectra (Fig. 5) because for the lower frequencies the spectra are mixed.

In vivo results with the new probes reveal that the microprobes may be used for rat brain blood flow monitoring. Blood perfusion variations promoted by nitrite intraperitoneal injection are clearly visible on the signals from both tested microprobes: the slight increment verified after the nitrite injection and the abrupt decrease observed in consequence of the cardiac arrest. In M1308 the typical signal obtained with Periflux 5000 cannot be seen in M1. However, a pattern that changes in accordance with the three regions can be seen. In general, signals collected with the microprobe have more electronic noise, when compared with the Periflux 5000 results. This indicates that improvements in the self-mixing acquisition channels must be done, namely the implementation of analogue and digital filters. For both acquisitions (M1308 and M785), the peak detected with the new prototype is close to the one obtained with Periflux 5000. Regarding the increase percentage, it is higher for the new probes. The smallest increase percentage obtained with the Perimed device in M785 may be due to the probe displacement.

Parameters used in this work, like sample frequency, frequency rate and filters cut-off frequencies, were based on the ones used in conventional laser Doppler flowmeters. However, for their validation, more tests with controlled parameters have to be carried out. Self-mixing interferometry devices have simple optical systems but self-mixing phenomena are complex. It is necessary to understand how the system responds to velocity and concentration of scatterers in order to use it in perfusion measurements. The variations of the back-coupled light intensity and its relation with the perfusion as well as the speckle statistical properties obtained from microcirculation blood flow must be understood [20, 21]. This is crucial to compare self-mixing sensors with the commercial sensors available.

Besides that, the absence of a calibration method is also a drawback. A proper calibration method could improve the microprobe response to slight changes in flow and a

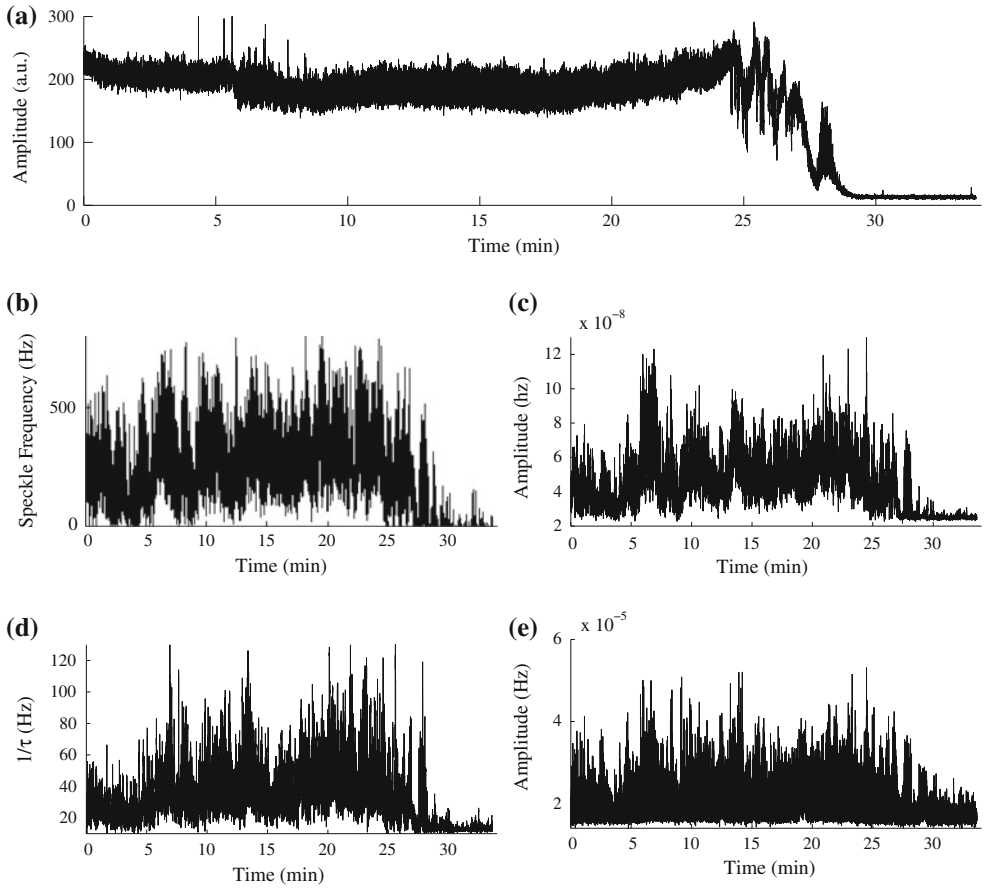

Fig. 8 In vivo validation results for M785: **a** Periflux 5000 results, **b** CM results, **c** AM results, **d** M0 results and **e** M1 results

more clear differentiation before and after cardiac arrest could be reached.

We present a novel miniaturized LDF probe based on a self-mixing method to monitor blood flow changes in deep brain structures. We show that the new probe can detect changes in the blood flow in the rat brain. However, improvements in the self-mixing acquisition channels must be done, namely the implementation of analogue and digital filters in order to reduce the electronic noise.

Acknowledgments The authors thank the "Instituto de Investigação Interdisciplinar (III)" of the University of Coimbra, "Acções Universitárias Integradas Luso–Francesas" (PAUILF) programme and "Fundação para a Ciência e a Tecnologia (FCT), Lisbon", for supporting this work. This work was carried out within the project PTDC-SAU-NEU-1017262008, developed under the scope of QREN initiative, UE/FEDER financing support, through the Programa Operacional Factores de Competitividade (COMPETE).

References

1. Bonner R, Nossal R (1981) Model for laser Doppler measurements of blood flow in tissue. Appl Opt 20:2097–2107
2. Fredriksson I, Fors C, Johansson J (2007) Laser Doppler flowmetry—a theoretical framework. http://www.imt.liu.se/bit/ldf/ldfmain.html
3. Fredriksson I, Larsson M, Stromberg T (2009) Measurement depth and volume in laser Doppler flowmetry. Microvasc Res 78:4–13
4. Haberl RL, Heizer ML, Marmarou A, Ellis EF (1989) Laser-Doppler assessment of brain microcirculation: effect of systemic alterations. Am J Phys 256:H1247–H1254
5. Hamberg LM, Hunter GJ, Kierstead D, Lo EH, González RG, Wolf GL (1996) Measurement of cerebral blood volume with subtraction three dimentional functional CT. AJNR Am J Neuroradiol 17:1861–1869
6. Humeau A, Steenbergen W, Nilsson H, Strömberg T (2007) Laser Doppler perfusion monitoring and imaging novel approaches. Med Biol Eng Comput 45:421–435
7. Iadecola C (2004) Neurovascular regulation in the normal brain and in Alzheimer's disease. Nat Rev Neurosci 5:347–360
8. Jonasz M (2011) Water structure and science. http://www.tpdsci.com/Tpc/AbsCfOfWaterQuerry1991.txt
9. Larson O (2006) Digital implementation of a Laser doppler perfusion monitor. Linköping, Electronics Systems
10. Meigas K, Inrikus H, Kattai R, Lass J (2003) Self-mixing in a diode laser as a method for cardiovascular diagnostics. J Biomed Opt 8:152–160
11. Mito K, Ikeda H, Sumi M, Shinohara S (1993) Self-mixing effect of the semiconductor laser Doppler method for blood flow measurement. Med Biol Eng Comput 31:308–310

12. Mul FFM, Koelink MH, Weijers AL, Greve J, Aarnoudse JG, Graaff R, Dassel ACM (1992) Self-mixing laser-Doppler velocimetry of liquid flow and of blood perfusion in tissue. Appl Opt 31:5844–5851
13. Mul FFM (2004) Monte-Carlo simulation of light transport in turbid media. In: Tuchin VV (ed) Handbook of coherent domain optical methods: biomedical diagnostics, environment and material science, chap 12, vol 2XLII (2-volume-set). Kluwer, Dordrecht , p 1004. ISBN:1-4020-7576-6
14. Oberg PA (1990) Laser-Doppler flowmetry. Crit Rev Biomed Eng 18:125–163
15. Oberg PA (2003) Optical sensors in medical care. Sens Update 13:201–232
16. Oliveira R, Semedo S, Figueiras E, Requicha Ferreira LF, Humeau A (2011) Laser Doppler flowmeters for microcirculation measurements. In: 1st Portuguese meeting in bioengineering—bioengineering and medical sciences—the challenge of the XXI century, Portuguese chapter of IEEE EMBS, Lisbon, pp 182-185
17. Ozdemir SK, Ito S, Shinohara S, Yoshida H, Sumi M (1999) Correlation-based speckle velocimeter with self-mixing interference in a semiconductor laser diode. Appl Opt 38:6859–6865
18. Ozdemir SK, Takasu T, Shinohara S, Yoshida H, Sumi M (1999) Simultaneous measurement of velocity and length of moving surfaces by a speckle velocimeter with two self-mixing laser diodes. Appl Opt 38:1968–1974
19. Ozdemir SK, Takamiya S, Ito S, Shinohara S, Yoshida H (2000) Self-mixing laser speckle velocimeter for blood flow measurement. IEEE Trans Instrum Meas 49:1029–1035
20. Ozdemir SK, Shinohara S, Takamiya S, Yoshida H (2000) Noninvasive blood flow measurement using speckle signals from a self-mixing laser diode: in vitro and in vivo experiments. Opt Eng 39:2574–2580
21. Ozdemir SK, Ohno I, Shinohara S (2006) Assessment on self-mixing laser interferometry for blood flow measurement over skin surface. Sorrento (Italy), pp 27–31
22. Ozdemir SK, Ohno I, Shinohara S (2008) A comparative study for the assessment on blood flow measurement using self-mixing laser speckle interferometer. IEEE Trans Instrum Meas 57:335–363
23. Paxinos C, Watson G (2007) The rat brain in stereotaxic coordinates. Academic Press, New York
24. Pinder AG, Pittaway E, Morris K, James PE (2009) Nitrite directly vasodilates hypoxic vasculature via nitric oxide-dependent and -independent pathways. Br J Pharmacol 157:1523–1530
25. Slot M, Koelink MH, Scholten FG, Mul FFM, Weijers L, Greve J, Graaff R, Dassel ACM, Aarnoudse JG, Tuynman FHB (1992) Blood flow velocity measurements based on the self-mixing effect in a fibre-coupled semiconductor laser: in vivo and in vitro measurements. Med Biol Eng Comput 30:441–446
26. Steinmeier R, Bondar I, Bauhuf C, Fahlbusch R (2002) Laser Doppler flowmetry mapping of cerebrocortical microflow: characteristics and limitations. Neuroimage 15:107–119
27. Tucker JR, Baque JL, Lim YL, Zvyagin AV, Rakić AD (2007) Parallel self-mixing imaging system based on an array of vertical-cavity surface-emitting lasers. Appl Opt 46:6237–6246
28. Zhang W, Ning YN (1996) Vibration-induced noise in a fiber lead of an optical current measurement system. Rev Sci Instrum 67:553–557
29. Zhang W, Ning YN, Grattan KTV, Palmer AW (1997) Analysis of the effect of vibration-induced noise in different fibre leads used in an optical current-measurement system. Sens Actuators A 63:113–118